7th International DAAAM Baltic Conference
"INDUSTRIAL ENGINEERING
22-24 April 2010, Tallinn, Estonia

FINITE ELEMENT ANALYSIS OF GAS BUBBLE INFLUENCE ON ULTRASONIC AIDED ELECTRODISCHARGE MACHINING

Ghiculescu, D.; Marinescu, N.I; Jitianu, Gh. & Jiga, G.

Abstract: *The paper deals with comparative influence of gas bubble duration formed around plasma channel on removal mechanism using Finite Element Analysis (FEA) under two different conditions: classic micro-electrodischarge machining (μEDM) and aided by ultrasonics (μEDM+US). FEA results regarding crater dimensions in case of μEDM emphasised that volume removed by discharge is roughly bordered by boiling isothermal due to long duration of gas bubble after pulse end. At μEDM+US, bubbles collective implosion from working gap can be exploited, increasing removal rate by more than 500% if this is produced within 0.5 μs from pulse end. More effective could be ultrasonic shock waves that remove the peaks of microgeometry, decreasing roughness up to 50% compared to classic μEDM.*
Key words: EDM, ultrasonics, gas bubble.

1. INTRODUCTION

The influence of gas bubble duration formed around plasma channel on removal mechanism is very important because only after its collapse, hydraulic forces are allowed to enter the vicinity of EDM spot and remove the melted material (fig.1).
Based on specific phenomenology, life time of gas bubble influence was studied by Finite Element Analysis (FEA) for classic micro-electrodischarge machining (μEDM) and ultrasonic aided micro-EDM (μEDM+US). Comsol Multiphysics, Transient Heat Transfer Module was used for modelling of thermal phenomena, specific to EDM, coupled with Structural Mechanics, Transient Analysis Module for modelling the mechanical stress produced by cavitational phenomena ultrasonically induced within working gap.
The goal of these researches is the optimization of μEDM+US in terms of machining rate and surface quality.

2. PHENOMENOLOGY AND WORKING PARAMETERS

The validation of many models attempting to evaluate the life duration is a difficult problem due to micrometric scale where these phenomena occur. The frontal working gap (s_F) at μEDM has less than 10 μm.
A basic model is Van Dijck's one, which in case of 1 A discharge current and 10 μs pulse time predicted that bubble life duration is around 180 μs [1], [2].
The validation of this model was achieved more recently using ultra speed cameras with more than 10^6 frames/s [3]. Thus, at such working parameters, gas bubble is much bigger than plasma channel and EDM spot, having dimensions of 0.1 mm order (fig. 1).

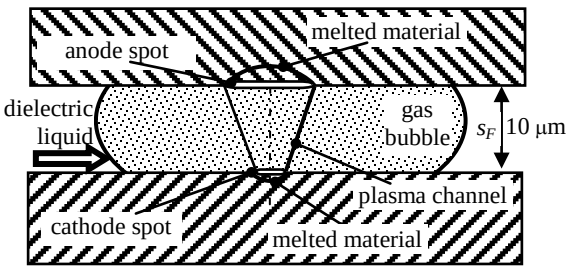

Fig. 1. Gas bubble dimensions during discharge at classic μEDM

FEA results validated by experimental data [4], [5], [6], also emphasised that plasma channel has a conical shape, narrowed next to cathode spot, approximately 2.5 times compared to anode spot.

In case of μEDM single discharge, the life time of gas bubble is prolonged, even after 120 μs from electrical breakdown of insulating medium, working with dielectric liquid based on n-dodecane [3]. After bubble implosion, no material removal is achieved because it is already solidified as it will be pointed out by FEA results. Only a clearing up of working gap is completed.

In real processes that comprise successive discharges, the life duration of gas bubble formed around plasma channel could be much shorted by following electrical discharge due to pressure created by new plasma channel development. This phenomenon is also sustained by the proximity where the next discharge occurs, which is determined by high conductivity of working medium produced by previous discharge. The dielectric liquid capacity from the gap can not be restored if pause time is not sufficient. Due to high volume of gas bubble compared to less than 10 μm gap (fig. 1), the next discharge could be produced in gaseous medium.

The life shortening of gas bubble is strongly dependent on ignition delay time (t_d). The following relation shows that t_d depends on other process parameters:

$$t_d \sim \frac{s_F^{\,3}}{k \cdot u_0^{\,2}} \qquad (1)$$

where: k is electrical conductivity of working liquid; u_o - ignition voltage, generally, a constant of EDM generator. Analyzing relation (1), it can be noticed that delay time is very sensitive to k. In case of micromachining, this could be expressed in relative long t_d, more than 100 μs as our experiments pointed out, due to low electrical conductivity [6]. This is the result of low discharge energy, specific to micromachining. So, in this case, at classic μEDM, life time of gas bubble could last long time after pulse end, and consequently a great amount of material could be already solidified by the time that hydraulic forces could access the EDM spot.

At (EDM+US), the electrode-tool vibrates on longitudinal (vertical axis - z) with ultrasonic frequency, usually 20 kHz, during machining. Consequently, cavitational phenomena are induced in the frontal gap. An acoustic pressure (p_{ac}) is created within dielectric liquid, which can be calculated with the relation:

$$p_{ac} = 2\pi \cdot c \cdot \rho \cdot f_{US} \cdot z \quad [\text{MPa}] \qquad (2)$$

where: c is sound velocity in dielectric liquid [m/s]; ρ - density of dielectric liquid [kg/m^3]; f_{US} - ultrasonic frequency [Hz]; z - electrode elongation [m], given by the relation:

$$z = A\sin\omega t \qquad (3)$$

where: A is oscillation amplitude [m]; $\omega = 2\pi f_{US}$[s^{-1}].

Total hydrostatic pressure (p_{ht}) also takes into account the local pressure (p_h) from the gap:

$$p_{ht} = p_{ac} + p_h \qquad (4)$$

The p_{ht} pressure variation along the elongation z is represented in fig. 2, based on relations (2-4) for amplitude A = 2 μm, enough to create cavitation.

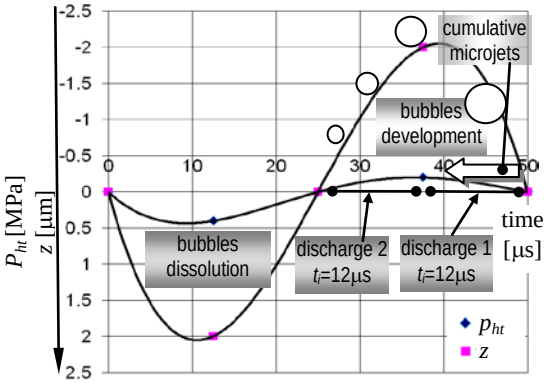

Fig. 2. Variation of hydrostatic pressure and tool elongation within the frontal gap at μEDM+US

Thus, p_{ac} was over cavitation threshold (p_{cav}) under our working conditions with dielectric liquid that has a density of 840 kg/m^3; p_h was considered 0.1 MPa.

From fig. 2, one can notice that capillary phenomena are produced in two semiperiods: liquid compression (bubbles dissolution in dielectric liquid) and liquid stretching (bubbles development) until cumulative microjets stage occurs. At each final stretching semiperiod, that lasts 25 μs in this case, collective implosion of bubbles from the gap is produced due to p_{ht} increase. Huge pressure of 10 MPa order is developed and shock waves parallel to machined surface decrease roughness by removing micropeaks with low shear resistance.

In case of total shutting down of gas bubble, Rayleigh provided the relation for calculation of implosion time (τ) [7]:

$$\tau = 0.915 R_m \sqrt{\frac{\rho}{p_h}} \quad [s] \qquad (6)$$

where R_m is maximum of bubble radius, depending on half ultrasonic period, $T_{US}/2$. Under our working conditions, τ was 0.84 μs. In this time interval, beside huge pressure, great temperature of around 10000 ^oC is developed. Thus, each bubble implosion has an equivalent effect of μEDM discharge, not damaging the surface quality. Only the shock waves pressure must be minimised not to increase *Ra* roughness as FEA results emphasised.

Some reference experimental data for FEA, registered when machining X210Cr12, tool steel on Romanian ELER 01 machine with commanded pulses, were synthesized in table 1, where I is current step, t_i – pulse time and t_0 – pause time.

Machining	EDM		EDM+US	
Crater dimensions	Depth [μm]	Radius [μm]	Depth [μm]	Radius [μm]
	3.6	4	1.6	3.2

Table 1. Craters mean dimensions obtained with commanded pulses, I=0.8A, t_i=12μs, t_0=6μs, positive polarity.

3. FEA MODELLING

The removal mechanism through commanded pulses was approached, obtaining temperature distribution after pulse end and after bubble collapse. The modelling addresses the synchronization between electrical discharges and the ultrasonic elongation of electrode-tool, related to collective implosion of bubbles ultrasonically induced in the gap (fig.2). Therefore only commanded pulses were considered due to their properties to have better timing control than relaxation ones.

At classic μEDM, the modelling cycle comprised heating by 12 μs pulse time (t_i), followed by 100 μs cooling time interval until next discharge occurs.

In the first stage, the geometry was created, working in 2D, aiming at computational resource saving, taking into account the symmetry of modelled phenomena (fig. 3). Preliminary modelling pointed out that initial shape of microgeometry introduces major errors. Thus, applying EDM spot on a flat surface produces crater depth of only 1.3 μm against of 3.6 μm under real conditions. The successive ellipses were generated by former discharges. The current EDM spot was applied on centre of microgeometry, i.e. x=[-4; 4] μm interval. The shape presents resolidified material on previous crater borders – volume with 0.5 μm diameter on the top of crater margin - due to difficult evacuation of material from a relative deep crater [8].

The workpiece was a square of 10 mm; previous runnings emphasised that dimensions of 10 mm order have no influence on temperature distribution. PT1 and PT2, on workpiece superior surface, defined the bubble gas dimensions of 0.1 mm order, around EDM spot.

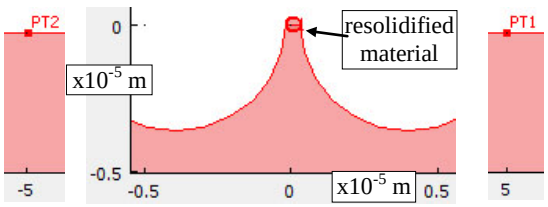

Fig. 3. The geometry parameters

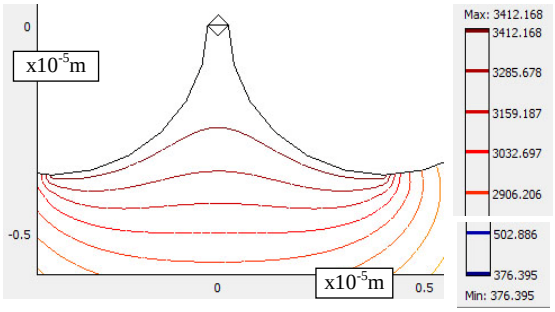

Fig. 4. Temperature [K] distribution after 12 μs commanded pulse

Meshing was based on Lagrange-T_2J_1 triangular elements. Thermal properties of X210Cr12 (D3 DIN) were loaded from Comsol Multiphysics library, all of them being temperature dependent.

As boundary settings, EDM spot has 3475K taking into account the assumption that during the pulse time the melted material is overheated above boiling temperature with 200-300^{o}C due to increased pressure produced by plasma channel [1]. The adjacent zones to EDM spot, bordered by PT1 and PT2 were considered as insulated due to gas bubble influence. The rest of boundaries belonging to workpiece were set at dielectric liquid temperature, i.e. 313 K.

At classic μEDM, temperature distribution from fig. 4 shows that a crater volume of 3.6 μm depth and 4.16 μm radius bordered by boiling isothermal (3273K), can be removed after 12μs pulse, very close to experimental data (table 1). The crater bottom shape has relatively irregular form due to boiling isothermal, whose position is dependent on initial microgeometry (fig.5).

After 100 μs from pulse end, when next discharge produces bubble collapse, melted material is almost completely cooled.

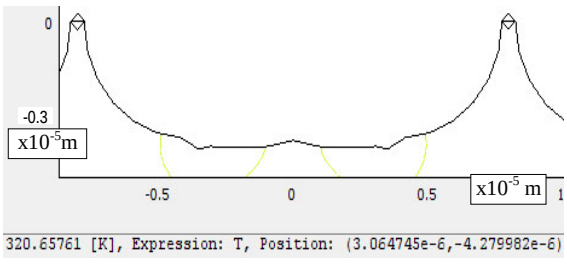

Fig. 5. Temperature [K] distribution after 100 μs from pulse end

Thus, no hydraulic removal is possible through dielectric liquid action, the material being in solid state. The temperature close to EDM spot is around 320K (fig.5), in agreement with Van Dicks' model [1], [2].

At μEDM+US, the modelling cycle comprised heating by 12 μs pulse time (t_i) (fig. 4) followed by cooling time interval until cumulative microjets stage occurs (fig.2). Two cases were considered: discharge 1 with cooling interval of only 0.5 μs and discharge 2 with cooling of 10 μs. In the first case, the pulse end is synchronised with bubbles collective implosion. Temperature distribution shows that a volume - ellipse with over 11 μm depth and 8.8 μm radius - bordered by 1683K isothermal, which is melting point of a steel with 2.1 % C and 12% Cr can be removed (fig. 6). Thus, even the margins of adjacent craters can be removed; this could be an increase of removed volume of more than 10 times compared to classic μEDM. This case is almost ideal concerning machining rate. Our experimental data emphasized that up to 500% machining rate growing can be obtained under some optimization conditions of working parameters [9].

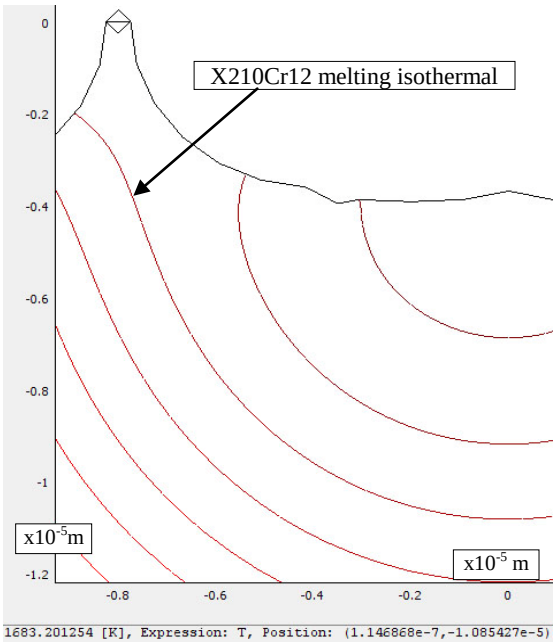

Fig. 6. Temperature [K] distribution at 0.5 μs after pulse end

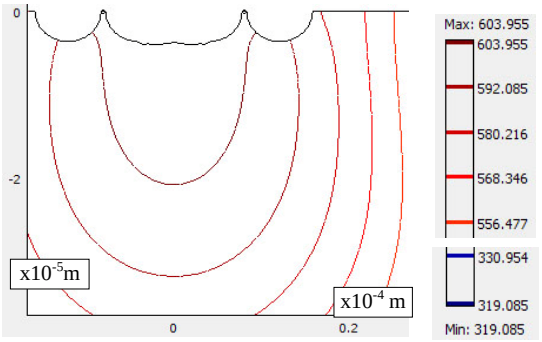

Fig. 7. Temperature [K] distribution at 10 μs after pulse end

The second modelled case, discharge 2 placed within US stretching semiperiod produced at 10 μs after pulse end - when collective bubbles implosion occurs - temperature distribution from fig.7. This emphasises that maximum temperature is under melting point; consequently, no hydraulic removal takes place. However due to pressure decrease during stretching semiperiod, the steel boiling point is lower with around 50K and the volume removed is greater than in case of classic μEDM.

The pressure produced by ultrasonic shock waves was also considered as additional removal mechanism. Stagnation pressure produced by cumulative microjets stage could lead to values of 10 MPa order during less than 1 μs [7]. Experimentally, the consumed power to actuate the acoustic chain at using of commanded pulses was greater with around 30 % than in case of relaxation pulses [9]. This is explained by the fact that craters margins produced by commanded pulses present resolidified material (fig.3), which are harder to remove.

Therefore, thermal transient analysis was coupled with mechanical homologous one, having temperature T as common variable and using same triangular elements.

As boundary conditions, follower load of 14 MPa (greater than in relaxation pulses case) was applied on the craters profile on x direction because US shock waves are oriented parallel to machined surface. Fixed constraints were applied on lateral and inferior sides of workpiece due to its fixing mode during machining.

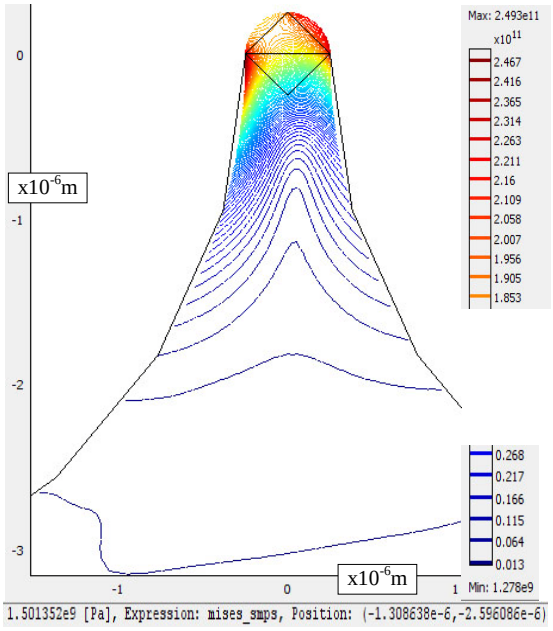

Fig. 8. Von Mises stresses [Pa] distribution within craters margins

The depth of volume removed by US shock waves was more than 2 μm (fig 8). X210Cr12 austenitized and tempered to hardness of 50 HRC had ultimate tensile strength of 1500 MPa [10]. Thus, the depth of crater could be reduced to more than 1.6 μm and its radius to 3 μm, close to experimental data from table 1. This is in agreement with our experimental data proving that roughness (R_a) of machined surface by EDM+US can be decreased with up to 50% compared to classic EDM if acoustic pressure (p_{ac}) is minimized. Nevertheless, it must be higher than cavitation threshold. So, optimum power to actuate US chain must be experimentally found for each machining type.

Other runnings show that at slight increase of follower load, a massive destruction of machined microgeometry could occur, indicating its high sensitivity to US shock waves. Moreover the width of crater margin has also a great influence on US removal. At greater width than present case, the follower load of collective bubbles implosion has no capacity to remove the crater margin. So, only when craters overlap is achieved (enough EDM time), i.e. crater margins having low width, ultrasonic removal becomes effective.

4. CONCLUSION

The results of FEA modelling of gas bubble influence are in agreement with experimental data, showing high increase of ultrasonic contribution to EDM machining rate and surface quality.

At classic microEDM, long life duration of gas bubble from the gap determines boiling as main material removal mechanism and consequently, low machining rate. After bubble collapse, the melted material is long time ago resolidified.

At microEDM+US, in order to take advantage on shorten bubble life time by US assistance, the collective bubbles implosion must occur within 0.5 μs from pulse end. However due to pressure decrease during stretching semiperiod inside the gap, the removed volume grows. This synchronization between discharges and tool elongation could increase machining rate more than 5 times.

More efficient is the additional removal mechanism by ultrasonic shock waves, decreasing roughness up to 50% by cutting microgeometry peaks. Then the power for actuating the ultrasonic chain is essential. Further researches will be focused on FEA results concerning ultrasonics contribution to EDM+US removal mechanism.

5. REFERENCES

1. Van Dijck, F., Snoeys, R., Theoretical and Experimental Study of the Main Parameters Governing the Electrodischarge Machining Process, *Mecanique*, 1975, **301-302**, p. 9-16.

2. Van Dijck, F., Snoeys, R., Metal Removal and Surface Layers in Electrodischarge Machining, *Int. Conf. On Prod. Eng. Proc*, 1974, Tokyo, Japan Soc. Prec. Eng, 46-50.

3. Schulze, H.-P. et al., Gas bubble morphology in small working gaps at spark erosion, 2004, *Available from:* http://eco.pepublishing.com/ *Accessed:* 2010-01-25.

4. Ghiculescu, D., Marinescu, N. I., FEM Simulation of Material Removal Mechanism at Ultrasonic Aided Electrodischarge Machining Finishing, *Proc. 19th Int. DAAAM Symposium, Slovakia*, 2008, 547-548.

5. Ghiculescu, D. Marinescu, N. I., Jitianu, G., Seritan, G., On precision Improvement by Ultrasonics-aided Electrodischarge Machining, *Estonian J. of Eng.*, 2009, **15, 1,** 24-33.

6. Marinescu, N. I., Ghiculescu, D. Jitianu, G., Solutions for Technological Performances Increasing at Ultrasonic Aided Electrodischarge Machining, *Int. J. Mater. Form.*, 2009, **2**, 681–684.

7. Anton, I. *Cavitation,* Romanian Academy Publishing House, Vol. I, II, Bucharest, 1985.

8. Ghiculescu, D. *Nonconventional Machining*, Printech, Bucharest, 2004.

9. Marinescu, N. I. et al. *Treatise of Nonconventional Technologies*, *Ultrasonics Machining*, Bren, Bucharest, 2004.

10. Farrahi, G.H., Ghadbeigi, H. An investigation into the effect of various surface treatments on fatigue life of a tool steel, *J. Mat. Proc. Tech*., 2006, *Available from:* http://www.sciencedirect.com/ *Accessed:* 2010-02-10.

6. ADDITIONAL DATA ABOUT AUTHORS

Ghiculescu, Daniel, Assoc. Prof., Ph.D.; e-mail: liviudanielghiculescu@yahoo.com

Marinescu, Niculae, Prof., Ph.D; e-mail: niculae.marinescu@yahoo.com

Jiga, Gabriel, Prof., Ph.D; e-mail: gabijiga@yahoo.com

"Politehnica" University of Bucharest; 313 Splaiul Independentei, sector 6, Bucharest, Romania, http://www.pub.ro; phone: 00404029373.

Jitianu, Gheorghe, Eng., SC Edming SRL, 4, Al. Lunca Siretului, sector 6, Bucharest, Romania, e-mail: gelu.jitianu@gmail.com, phone:0040072348513.